33RD INTERNATIONAL COSMIC RAY CONFERENCE, RIO DE JANEIRO 2013
THE ASTROPARTICLE PHYSICS CONFERENCE

ICRC 2013

Measurement of the atmospheric ν_μ spectrum with IceCube 59

THE ICECUBE COLLABORATION[1],

[1]*See special section in these proceedings*

tim.ruhe@udo.edu

Abstract: The energy spectrum of the atmospheric muon neutrino flux was measured with the IceCube detector in the 59-string configuration, using an unfolding procedure. This measurement extended IceCube's reach for atmospheric neutrinos up to 1 PeV in energy. This extension in energy was obtained by using a machine learning algorithm preceeded by a dedicated feature selection for event selection, and by applying the novel unfolding algorithm TRUEE.

Corresponding authors:
Tim Ruhe[1],
[1] *Lehrstuhl für Experimentelle Physik V, Technische Universität Dortmund*

Keywords: Atmospheric neutrinos, IceCube, Unfolding.

1 Introduction

IceCube is a state of the art neutrino telescope located at the geograophic South Pole. Its 5160 Digital Optical Modules (DOMs) are mounted on 86 vertical cables called strings, thus forming a three dimensional array of photosensors [1].
Although primarily designed for the detection of high energy neutrinos from astrophysical sources, the detector can be utilised for various other studies, including measurements of the atmospheric neutrino spectrum. Despite the fact that the atmospheric neutrino spectrum was already measured by various experiments, including AMANDA [2] and IceCube in the 40-string configuration [3], the flux at high energies is still subject to rather large uncertainties [4].
The flux of atmospheric muon neutrinos is dominated by neutrinos originating from the decay of pions and kaons, produced by cosmic-ray interactions in the atmosphere, up to engergies of $E_\nu \approx 100$ TeV [2]. Due to their relatively long lifetime pions and kaons lose part of their energy in collisions prior to decaying. The atmospheric neutrino spectrum is therefore expected to follow a power law one power steeper (asymptotically $\frac{d\Phi}{dE} \propto E^{-3.7}$) compared to the spectrum of primary cosmic rays [3].
At energies exceeding 500 TeV neutrinos from the decay of charmed mesons are expected to contribute notably to the spectrum. Due to their short lifetime ($t_{\text{life}} \approx 10^{-12}$ s [5]) these mesons decay before interacting and follow the intial spectrum of cosmic rays more closely, therefore causing a flattening of the overall neutrino flux [2, 3].
As neutrinos cannot be detected directly, neutrino induced muons produced in charged current interactions are used for a measurement of the atmospheric neutrino flux.
Atmospheric muons, produced in cosmic-ray interactions as well, enter the detector from above, thus forming a significant background in the searches for atmospheric neutrinos. As the number of atmospheric muons exceeds the number of neutrino induced muons by several orders of magnitude, a detailed event selection needs to be carried out in order to obtain a high purity neutrino event sample. Within the analysis presented here, a machine learning based event selection was used. Details on this approach are given in the next section.
Although IceCube was finished in December 2010, data was already taken in previous detector configurations. Data for this analysis were taken between May 2009 and May 2010 in the 59-string configuration of the detector.

2 Event Selection

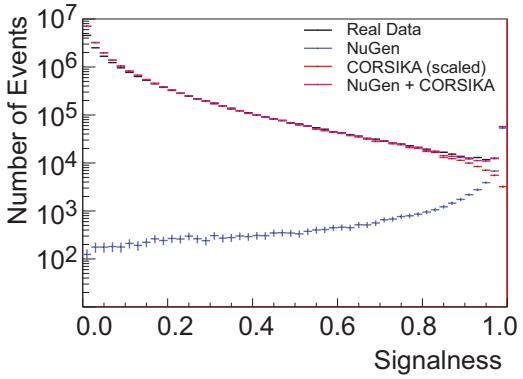

Fig. 1: Random Forest output score (signalness) for signal simulation (blue) generated using the IceCube neutrino generator NUGEN and background simulation (red) generated with CORSIKA [10]. Real data is shown in black, whereas the sum of simulated signal and background events is depicted in magenta. The sum of simulated signal and background events is found to agree well with the distribution of real data, indicating a stable performance of the Random Forest.

The event selection used in this analysis consisted of three basic steps, the first one being the application of quality cuts. These quality cuts were followed by a detailed algorithm based feature selection, aiming at the identification of reconstructed track parameters to be used

for the training of a Random Forest [8]. The training and testing of the Random Forest was carried out as a third step.

The afore mentioned quality cuts were simultaneously applied to the LineFit velocity ($v_{LineFit} > 0.19$) and the reconstructed zenith angle ($\theta > 88^\circ$). The LineFit velocity is the estimated velocity of the lepton, obtained by fitting a straight line to the spatial and time-distribution of detected light. Cascade like events, originating from charged current ν_e interactions and neutral current interactions of all neutrino flavors, will produce a spherical light pattern, from which small values of $v_{LineFit}$ are reconstructed. Larger values of $v_{LineFit}$ are obtained for track-like events from ν_μ CC interactions. The selection of high quality track-like events is required in order to obtain rather long tracks, from which the energy of the incoming neutrino can be reliably reconstructed.

The zenith-angle cut is mainly aimed at reducing the contamination of atmospheric muons entering the detector at angles $\theta < 90^\circ$. Choosing a cut at $\theta > 88^\circ$ rather than at $\theta > 90^\circ$ aims at slightly extending the field of view in order to detect higher energy neutrinos from above the horizon.

The quality of an automated, machine learning based, event selection largely depends on the utilised set of event parameters. In machine learning, these event parameters are often referred to as features or attributes. As not all attributes are equally well suited for the event selection, a representation in fewer dimensions needs to be found. In general, utilising knowledge about the detector and the classification problem at hand, will result in a good set of features that can be used for the training of a classification algorithm. It will, however, not necessarily result in the *best* set of features.

The Minimum Redundancy Maximum Relevance (MRMR) algorithm [6] was used for the selection of features. Using MRMR is particularly useful when certain quanities (e.g. zenith angle) are obtained from a number of different reconstruction algorithms.

Prior to running MRMR, a number of attributes, which were known to be either useless, redundant, or a source of potential bias, were excluded by hand. This mainly concerned timing information and sky coordinates. All event selection steps regarding machine learning and data mining were carried out using the RAPIDMINER [7] machine learning environment.

Twenty-five attributes were selected in the final event selection as this number represents a reasonable tradeoff between feature selection stability and the anticipated complexity of the learner. Three additional attributes were created and added to the attribute set, according to the findings presented in [3].

A Random Forest [8], which utilises an ensemble of simple decision trees, was chosen as a learning algorithm. Tree based algorithms are well known for their stability and interpretability and were found to perform well in previous IceCube analyses [3]. Moreover, Random Forests were found to outperform other classifiers in [9]. The forest was trained and tested in a five-fold cross validation utilising 70,000 simulated neutrino events and 750,000 simulated background events. The neutrino events were generated by the IceCube neutrino generator NUGEN, according to an E^{-2} spectrum in order to provide a sufficient number of examples at high energies. Background events were simulated according to the poly-gonato model using CORSIKA [10]. In order to avoid overtraining, the number of examples used for the trainig of the forest was limited to 27,000 signal and background events, respectively. The ratio of signal to background events was set at 1:1 in the training process. Although the true distribution of signal and background events differs strongly from 1:1 on real data (93,000 neutrinos in 17.48×10^6 background events), tests showed that this ratio provided a reasonable tradeoff between signal efficiency and background rejection.

The Random Forest output score (signalness) for simulated signal events (blue) and simulated background events (red) is shown in Fig. 1. Real data is shown in black, whereas the sum of signal and background simulation is depicted in magenta. The sum of simulated signal and background events is found to agree well with the distribution of real data, indicating a stable performance of the Random Forest.

The application of the Random Forest on the full set of IC-59 data was found to yield 27,771 neutrinos in 346 days of IC-59 (80 neutrino events per day). Compared to an expectation of 29,884 neutrino events, derived from Monte Carlo simulations, a slight underfluctuation is observed. This underfluctuation, however, is found to be well within the estimated systematic uncertainties of the event selection. The purity of the final neutrino event sample was estimated to be 99.6%. It should be noted, that no events with a zenith angle $\theta < 90^\circ$ were observed in the sample, after the application of the Random Forest.

3 Spectrum Unfolding

As the neutrino energy spectrum cannot be accessed directly, it needs to be inferred from the reconstructed energy of the muons. This task is generally referred to as an inverse- or ill posed problem and described by the Fredholm integral equation of first kind [11]:

$$g(y) = \int_b^a A(y,E)\, f(E)\, dE. \tag{1}$$

For the discrete case this is transformed into:

$$\vec{g}(y) = \underline{A}(E,y)\, \vec{f}(E), \tag{2}$$

where $\vec{f}(E)$ represents the sought energy distribution, whereas the measured energy dependent distribution is given as $\vec{g}(y)$. $\underline{A}(x,E)$ represents the response matrix of the detector, which also accounts for the physics of neutrino interactions in or near the detector as well as for the propagation of the muon.

Several approaches to the solution of inverse problems exist. The unfolding program TRUEE [11], which is an extension of the well known $\mathscr{RUN}$ [12] algorithm, was used for unfolding in this analysis.

Five unfolding settings (three different sets of input variables and two different settings for the regularisation parameter) were found to produce stable results, when tested on Monte Carlo simulation. Compatible results were obtained for all of these five settings, when applied to real data. The setting least sensitive to the ice model was chosen for the final unfolding (see section 4), in order to keep the systematic uncertainties as small as possible.

Three variables (track length, number of channels, number of direct photons) were used as input for the unfolding as TRUEE allows for the use of up to three input parameters.

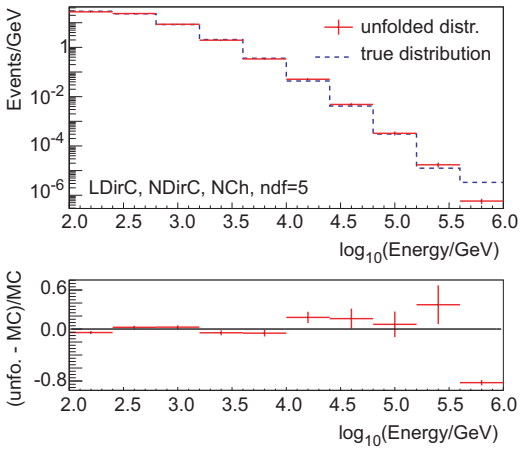

Fig. 2: Selected test mode result. The true distribution is represented by the blue dashed line, whereas the unfolding result is depicted by the red line. A good agreement between both distributions is observed.

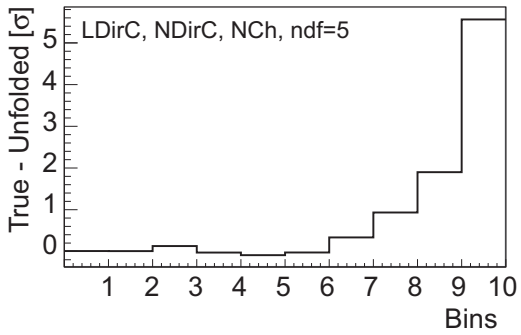

Fig. 3: Average deviation of the unfolding result from the true distribution in units of the statistical uncertainty σ. Only small deviations are observed for the first eight bins. The discrepancies are found to increase towards higher energy, due to the steeply falling spectrum of atmospheric neutrinos.

In IceCube, photons are considered direct when they are detected within a certain time window, computed with respect to the reconstructed track. An estimate of the track length inside the detector is obtained by projecting all DOMs that recorded direct photons onto the reconstructed track. The number of channels corresponds to the number of DOMs hit during an event.

Good data to Monte Carlo agreement, as well as good correlation with energy were observed for all variables. The stability of the unfolding as well as the results obtained on real data are addressed in the following.

A selected test mode result comparing the unfolding result to the true distribution of events is shown in Fig, 2. The true distribution is represented by the blue dashed line, whereas the unfolding result is shown in red. In general both distributions were found to agree well. Discrepancies were observed for the last bin. Whether this poses a potential problem to the stability of the result cannot be determined from the outcome of a single unfolding.

The stability of the unfolding was validated in a bootstrapping procedure implemented in the pull mode of TRUEE. Within this pull validation 500 test unfoldings were carried out, each treating 30,000 events as pseudodata. For all of these unfoldings, the deviation between the unfolding result and the true distribution is computed

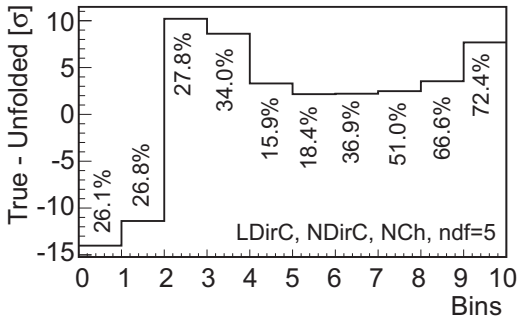

Fig. 4: Estimated systematics due to uncertainties in the ice model obtained by applying the pull mode on a different set of Monte Carlo simulations. The deviation between the unfolding result and the true distribution in units of the statistical uncertainty is depicted on the y-axis. Systematic uncertainties of the order of 30% are observed for the first couple of bins. Larger errors are observed towards higher energies.

binwise and in units of the statistical uncertainty σ [11]. The average deviation of the individual bins is shown in Fig. 3. Only small deviations (well below the 1σ limit) were observed for the first seven bins, indicating a stable behaviour of the unfolding.

The rather large deviation obtained for the highest energy bins is a result of the steeply falling spectrum of atmospheric neutrinos and the bootstrapping procedure applied in the pull mode. Due to the small number of events in the last bin, either 0 or 1 events are drawn randomly from the true distribution. Two or more events are only drawn in rather rare cases. Based on the response matrix, which accounts for the limited statistics in the highest energy bins by using ten times more events compared to real data, only a fraction of an event is reconstructed for the highest energy bin. As the statistical uncertainties derived in TRUEE fail to cover the distance of the predicted bin content to the true bin content, large deviations are observed. This further implies that an overestimation is obtained in case no events are present in the last bin on real data. An underestimation is observed in case one event is present in this bin in real data. As there is no way to determine the number of events in the last bin on real data prior to unblinding, the statistical uncertainty for the last bin should cover both of the cases discussed above. The pull mode in TRUEE, therefore, simultaneously serves as a cross check for the size of the statistical uncertainties derived as part of the algorithm.

Thus, taking into account the pull mode results for the last and next to last bin, one finds that the uncertainties derived in TRUEE are estimated too small for these two bins, as possible statistical fluctuations in real data are not covered. The statistical uncertainties of these bins were, therefore, scaled up by 1.9 and 5.56, respectively.

The normalisation of the atmospheric flux, as well as the spectral index were found to be retained during the unfolding.

4 Estimation of Systematic Uncertainties

Since the pull mode in TRUEE can be used on two different sets of Monte Carlo simulation, it offers the possibility to study systematic effects in a statistically reliable manner. Within this study the Monte Carlo set used for the determination of the response matrix is kept

constant with respect to the unfolding of real data. Monte Carlo sets differing in certain systematic parameters were then treated as pseudodata. Similar to the pull mode discussed above, these pseudodata were unfolded 500 times and the deviation between the unfolding result and the true distribution was calculated in units of the statistical uncertainty. The obtained deviation can be easily converted into a relative uncertainty, as the statistical uncertainty returned by the unfolding algorithm was found to vary by less than 2% level between different unfoldings.

One of the main sources of systematic uncertainties is the modelling of the ice used in the Monte Carlo production. The outcome of using the pull mode on simulation generated with different ice models is shown in Fig. 4. Error bars on the order of 30% or below are observed for the first seven bins. The uncertainties were found to increase in the highest energy bins. One should note that large uncertainties in units of the statistical uncertainty correspond to rather small relative errors in the first bins. This behaviour is due to the large statistics obtained in the first couple of bins, which in turn leads to rather small statistical errors.

An increase and decrease in the pair production cross section, respectively, was used to investigate the effect of uncertainties on the amount of light detected in IceCube. As the observation of more or less light, respectively, can in principle be caused by various effects that cannot be disentangled on real data, a double counting of the same systematic uncertainty needs to be avoided.

Cross checks on the size of the systematic uncertainty were performed by dividing the detector into two distinct subdetectors according to the z-coordinate of the center of gravity of the charge distribution of the event (COGZ). COGZ is calculated with respect to the center of the detector. In these checks the detector is split up into an inner and an outer layer, which aims at maximizing the difference in the ice for both detectors. The inner layer, which contains a large layer of dust, contains all events for which COGZ $> -225\,\mathrm{m}$ and COGZ $\leq 225\,\mathrm{m}$. The outer layer of the detector contains all events for which COGZ $\geq 275\,\mathrm{m}$ or COGZ $\leq -275\,\mathrm{m}$. Buffer zones of 50 m were introduced between the subdetectors in order to avoid a random counting of events into one of the subdetectors due to small uncertainties in the ice.

This cross check yielded very positive results, as the observed spectrum obtained using the full IceCube detector was found to agree with the two subdetector spectra within the estimated systematic uncertainties. This result was confirmed by an additional cross check, which divided the detector into an upper- and a lower layer. It can therefore be concluded that the systematic uncertainties have been correctly and reliably estimated.

5 Final Result

Figure 5 shows the zenith-averaged and acceptance corrected flux of atmospheric neutrinos obtained with IceCube in the 59-string configuration. Two theoretical model calculations are shown for comparison. The model using Honda et al. [13] (conventional) and Enberg et al. [14] (prompt) is depicted in red, wheras the conventional model by Barr et al. [15] is shown in black.

Good agreement between the measured flux of atmospheric neutrinos and the model calculations is observed. The systematic uncertainties have been reduced, compared to previous measurements of the atmospheric neutrino flux with IceCube, especially in the intermediate energy region. Furthermore, a measurement of the atmospheric neutrino flux up to an energy of 1 PeV was obtained. Thus, the energy range accessible using the IceCube detector has been extended from 400 TeV to 1 PeV compared to a measurement obtained using IceCube in the 40-string configuration [3].

No statement on a possible contribution of neutrinos from the decay of charmed mesons can be made, due to the limited statistics and large systematic uncertainties in the high energy region.

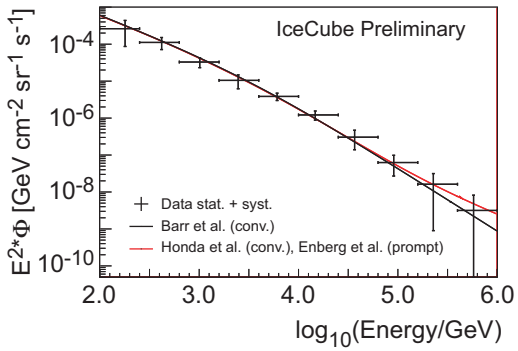

Fig. 5: Acceptance corrected and zenith-averaged atmospheric neutrino spectrum obtained with IceCube, compared to theoretical predictions. The model using Honda al. [13] (conv.) and Enberg et al. [14] (prompt) is depicted in red. The conventional model by Barr et al. [15] is shown in black. Good agreement between the unfolded flux and the theoretical models is observed. No statements on a contribution of neutrinos from the decay of charmed mesons can be made due to the rather large systematic uncertainties in the highest energy bins.

References

[1] T. DeYoung, Modern Physics Letters A 24 (2009) 1543.
[2] R. Abbasi et al, Astroparticle Physics 34 (2010) 48.
[3] R. Abbasi et al., Physical Review D 83 (2011) doi:10.1103/PhysRevD.83.012001.
[4] A. Fedynitch et al., Physical Review D 86 (2012) 114024.
[5] J. Behringer et al. (Particle Data Group), Physical Review D 86 (2012) 010001.
[6] C.H.Q. Ding and H. Peng, Journal of Bioinformatics and Computational Biology 3 (2005) 185.
[7] S. Fischer et al., Technical Report CI-136/02 Collaborative Research Center 531 (2002) 1.
[8] L. Breiman, Machine Learning 45 (2001) 5.
[9] R.K. Bock et al., Nuclear Instruments and Methods in Physics Research A 516 (2004) 511.
[10] D. Heck et al., Technical Report Forschungszentrum Karlsruhe GmbH (1998) 1.
[11] N. Milke et al., Nuclear Instruments and Methods in Physics Research A 697 (2013) 133.
[12] V. Blobel, Technical Note TN361 OPAL (1996) 1.
[13] M. Honda et al., Physical Review D 75 (2007) 043006.
[14] R. Enberg et al., Physical Review D 78 (2008) 043005.
[15] G.D. Barr et al., Physical Review D 70 (2004) 023006.